

Distribution Fitting for Combating Mode Collapse in Generative Adversarial Networks

Yanxiang Gong, *Student Member, IEEE*, Zhiwei Xie, Guozhen Duan, Zheng Ma, Mei Xie

Abstract—Mode collapse is a significant unsolved issue of generative adversarial networks. In this work, we examine the causes of mode collapse from a novel perspective. Due to the nonuniform sampling in the training process, some sub-distributions may be missed when sampling data. As a result, even when the generated distribution differs from the real one, the GAN objective can still achieve the minimum. To address the issue, we propose a global distribution fitting (GDF) method with a penalty term to confine the generated data distribution. When the generated distribution differs from the real one, GDF will make the objective harder to reach the minimal value, while the original global minimum is not changed. To deal with the circumstance when the overall real data is unreachable, we also propose a local distribution fitting (LDF) method. Experiments on several benchmarks demonstrate the effectiveness and competitive performance of GDF and LDF.

Index Terms—Generative Adversarial Nets, mode collapse, nonuniform sampling, distribution fitting

I. INTRODUCTION

GENERATIVE adversarial networks (GANs) [13] have attracted much attention since the first introduction. Owing to its excellent performance, this adversarial training scheme became one of the most significant achievements in the machine learning field of the past decades. The framework simultaneously trains two sub-networks: a generator that generates samples from a noise vector and a discriminator designed to distinguish real and fake samples. In the optimal case, the generated samples cannot be discriminated from the real ones. However, GAN training is dynamic and sensitive to nearly every aspect of its setup, from optimization parameters to model architecture [4]. Thus, GANs encounter challenges in the training process. Mode collapse is one of the main obstacles, which represents that GANs may fail to model the full distribution and some minor modes might not be captured. Even a simple Gaussian mixture model can work better than GANs on capturing the underlying distribution and provides an explicit representation of the statistical structure [36]. To address the issue, researchers presented various methods, including applying multi-generators [12], [23], improving the training strategy [31], [43], [45], [46], using penalty modules [2], [7], [25], [34], [41] and adding constraints [1], [10], [11], [15], [19], [26], [29], [30], [32], [44]. There are also methods for unbalanced or very small samples under different

categories [14], [38], [47]. However, mode collapse remains a troublesome issue in complicated applications of GANs. Researchers are still working hard on it [6], [22], [27], [28], [48]. Therefore, the study of methods for combating mode collapse remains of great importance.

In GANs [13], the output of the discriminator represents the probability that the input sample came from the real data. The authors demonstrated that the generator's global minimum under the optimal discriminator is reached if and only if the generated distribution is the same as the real one. However, we notice that the minimum value is also reachable while the generated and real distributions are not the same due to the nonuniform sampling in the training process. In this case, the sampled distribution cannot adequately denote the complete real distribution, and the GAN objective can occasionally reach the minimum in practical training. As a result, the risks of mode collapse will increase and GAN training will be sensitive, requiring us to adjust each parameter carefully. Therefore, we consider that the nonuniform sampling issue is one of the reasons which leads to mode collapse. However, the existing techniques mostly aim at other aspects of the mode collapse issues, which cannot handle the mentioned problem well. Meanwhile, some disadvantages are also obstacles to applications of the existing methods, such as heavy computation, requirements of manual design, and lack of interpretability. Thus, related research on this problem is still valuable and indispensable.

In this work, we propose a global distribution fitting method to combat the mode collapse problem. We design a penalty to constrain the generated data's distribution and incorporate it into the training objective. We prove that on the basis of not changing the global minimum of the GAN objective, the method will make it harder to reach the minimum value while the generated and real distributions are not the same. Furthermore, to cope with situations where the overall real data is unreachable, we propose a local distribution fitting method, utilizing sampled distribution to match the real one. The proposed methods will not bring heavy computation or require complicated manual design, making it easy to implement them in other frameworks. The experiments on several benchmarks demonstrate the effectiveness and competitive performance. To summarize, there are three main contributions in this work:

- We analyze the causes of mode collapse from a new perspective. Because of the nonuniform sampling in practical training, the GAN objective could reach the minimum value when the generated and real distributions are not

Corresponding author: Mei Xie.

The authors are with the School of Information and Communication Engineering, University of Electronic Science and Technology of China, Chengdu 611731, China (e-mail: yxgong@std.uestc.edu.cn; xiezhiwei@std.uestc.edu.cn; 202022011405@std.uestc.edu.cn; zma@uestc.edu.cn; mxie@uestc.edu.cn).

the same. Therefore, the training will be sensitive and risks of mode collapse will increase.

- We propose global and local distribution fitting methods to suppress mode collapse. On the basis of not changing the global minimum of the GAN objective, the method will make the objective harder to reach the minimum when the generated distribution is not the same as the real one.
- We demonstrate the effectiveness of the proposed method with both theoretical derivation and experiments. The theorems and proofs are also of great reference value for other methods based on distribution or feature matching.

II. RELATED WORK

Research on mode collapse problems has been an attractive field in recent years. Existing methods can be roughly classified into four categories: applying multi-generators, improving training, using penalty modules, and adding constraints. Each kind of method is effective and aims at different aspects of the issue.

A. Applying Multi-Generators

A simple but effective method is to apply multi-generators in GANs. For instance, Ghosh *et al.* [12] proposed to utilize multi-generators to generate different data. Li *et al.* [23] also applied multiple generators to learn the mapping from the randomized space to the original data space. The performance is excellent, but a manual design is required for the number of generators. Therefore, these methods can be used to maximum advantage in tasks where the mode number is known.

B. Improving Training

Some researchers tried to improve the training strategies to suppress mode collapse. Metz *et al.* [31] proposed to "unroll" the optimizer to suppress mode collapse. Tolstikhin *et al.* [43] borrowed some ideas from AdaBoost to address the problem of missing modes. Wang *et al.* [45] proposed an optimization method named Langevin Stein Variational Gradient Descent to stabilize the training. You *et al.* [46] proposed to optimize the model with maximum a posteriori estimation. The advantage of these methods is that they only change the training strategy, so they can be easily applied in any framework. However, additional computation will be required, and thereby they might not be efficient under restricted hardware conditions.

C. Using Penalty Modules

Using penalty modules is also an idea for suppressing mode collapse. The central idea of these methods is to penalize the generator when the generated data diversity is insufficient. Srivastava *et al.* [41] featured a reconstructor network to reverse the action of the generator by mapping from data to noise. Lin *et al.* [25] modified the discriminator to make decisions based on multiple samples from the same class, which penalizes generators with mode collapse. Chong *et al.* [7] utilized a regularizer to penalize the mini-batch variance. Pei *et al.* [34] introduced a pluggable diversity penalty module to enforce the

generator to generate images with distinct features. Bang *et al.* [2] leveraged a guidance network to induce the generator to learn the overall modes. The methods directly require the generated data to be diverse, which achieve competitive performance.

D. Adding Constraints

Adding constraints is another simple and effective way to suppress mode collapse. Arjovsky *et al.* [1] first proposed to clip the gradient to satisfy Lipschitz continuity. This idea brought lots of related research. Then Gulrajani *et al.* [15] improved the method by introducing gradient penalty, which is more stable. Kodali *et al.* [19] also proposed to introduce the penalty to limit the gradient around some real data points. Miyato *et al.* [32] proposed to constrain the spectral norm of each network layer to control the Lipschitz constant. Liu *et al.* [26] found an issue of spectral collapse and proposed a method to alleviate the issue. Mescheder *et al.* [30] analyzed the regularization strategies and proved local convergence for simplified gradient penalties. Ge *et al.* [11] introduced the clustering regularization term in the network to avoid mode collapse. The aim of these methods is to limit the gradient because the gradient will be sharp when mode collapse occurs [19].

In addition to limiting gradients, other constraints were also applied. Tran *et al.* [44] proposed a distance constraint to enforce compatibility between the latent sample distances and the corresponding data sample distances. Mao *et al.* [29] proposed maximizing the distance ratio between generated images. Eghbal-zadeh *et al.* [10] encouraged the discriminator to form clusters, which will lead the generator to discover different modes. Compared to limiting gradients, these methods explicitly specify the generated diversity. In this work, we propose a new constraint from a novel perspective. The parameters of the real and generated distributions are constrained to be almost the same. Thus, to maintain the consistency of parameters, the data modes cannot be missed.

III. ANALYSIS OF MODE COLLAPSE

The training objective of the original GANs [13] is

$$\min_G \max_D V(D, G) = \mathbb{E}_{\mathbf{x} \sim p_{data}(\mathbf{x})} [\log(D(\mathbf{x}))] + \mathbb{E}_{\mathbf{z} \sim p_z(\mathbf{z})} [\log(1 - D(G(\mathbf{z})))] \quad (1)$$

where \mathbf{x} is a real sample and \mathbf{z} is a random noise vector. The authors have demonstrated that the optimal D is

$$D_G^*(\mathbf{x}) = \frac{p_{data}(\mathbf{x})}{p_{data}(\mathbf{x}) + p_g(\mathbf{x})} \quad (2)$$

where p_{data} denotes the real data distribution and p_g denotes the generated data distribution. The virtual training criterion

$$C(G) = \max_D V(D, G) \quad (3)$$

which is a Jensen–Shannon divergence, will reach the global minimum $-\log(4)$ when $p_g = p_{data}$. At that point, $D_G^*(\mathbf{x}) = \frac{1}{2}$. In later studies, there are also improved frameworks that utilized Wasserstein distance [1], [15] or Hinge loss [24],

which are also proven to reach the minimum if and only if $p_g = p_{data}$ and effectively learn the distribution.

However, there may be some issues. Because we use a sampled batch of data whose distribution is p_s to replace p_{data} in practical training, nonuniform sampling may occur in some cases. Thus, we conjecture that the minimum value can be reached when $p_g \neq p_{data}$ in some cases.

First, we will give the mathematical definition of nonuniform sampling. The prerequisite of nonuniform sampling is that p_{data} is a mixed distribution that consists of $\phi(\mathbf{x}) = \{\phi_1(\mathbf{x}), \phi_2(\mathbf{x}), \dots, \phi_K(\mathbf{x})\}$, $K > 1$, which can be linearly expressed as

$$p_{data}(\mathbf{x}) = \sum_{k=1}^K \alpha_k \phi_k(\mathbf{x}) \quad (4)$$

where $\alpha_k \in (0, 1)$ is the weight of the k -th sub-distribution.

Definition 1. *In one training iteration of GANs, if each real data in a batch is sampled from one of, or the combination of several sub-distributions $\{\phi_m(\mathbf{x}), \phi_{m+1}(\mathbf{x}), \dots, \phi_n(\mathbf{x})\}$ of p_{data} , where $1 \leq m \leq n \leq K$ and $n - m < K - 1$, nonuniform sampling occurs.*

According to the definition, it can be observed that some sub-distributions are missed when nonuniform sampling occurs because no data is sampled from them. Thus, the training objective can reach the minimum in some iterations when $p_g \neq p_{data}$.

Lemma 1. *In the training process of GANs, $C(G)$ can sometimes reach the minimum even if $p_g \neq p_{data}$.*

Proof. In one training iteration of GANs, we will sample a batch of data to represent p_{data} , whose distribution is p_s . When nonuniform sampling occurs, the sampled data distribution can be expressed as

$$p_s(\mathbf{x}) = \sum_{k=m}^n \beta_k \phi_k(\mathbf{x}) \quad (5)$$

where $\beta_k \in (0, 1)$ is the weight of the k -th sub-distribution. Obviously, it is possible that $p_s \neq p_{data}$ because $n - m < K - 1$. Then if p_g only learns the sampled distribution which achieves $p_g = p_s$, $C(G)$ will reach the minimum when $p_g \neq p_{data}$. \square

Lemma 1 indicates that GAN loss can reach the minimum when the generator is not well trained. In this case, the generator only learns a part of the real distribution, which brings risks of mode collapse. We can identify several circumstances where nonuniform sampling is more likely to occur based on the lemma.

Theorem 1. *In the training process, nonuniform sampling is more likely to occur when the overlaps between sub-distributions are smaller.*

Proof. In p_{data} , when there is an overlap between several sub-distributions, a data sample can be sampled from their combination. Without loss of generality, assume that p_{data} has only two sub-distributions that contain an overlap. Use $\mathbf{x} \in overlap$ to represent \mathbf{x} is sampled from the combination of the

two sub-distributions, and then the probability can be marked as $P(\mathbf{x} \in overlap | \mathbf{x} \in p_{data})$.

If nonuniform sampling occurs, each data in a real data batch should be sampled from one sub-distribution according to the definition. The probability that all samples are from one sub-distribution is

$$\begin{aligned} & \prod_{i=0}^b P(\mathbf{x}_i \notin overlap | \mathbf{x}_i \in p_{data}) \\ &= \prod_{i=0}^b [1 - P(\mathbf{x}_i \in overlap | \mathbf{x}_i \in p_{data})] \end{aligned} \quad (6)$$

where \mathbf{x}_i is the i -th sample in a batch and b is the batch size. If the overlaps between sub-distributions are smaller, we will have $P(\mathbf{x}_i \in overlap | \mathbf{x}_i \in p_{data}) \rightarrow 0$, which indicates $P(\mathbf{x}_i \notin overlap | \mathbf{x}_i \in p_{data}) \rightarrow 1$. Therefore, the probability that all samples are from one sub-distribution is larger, and nonuniform sampling is more likely to occur. It is not difficult to generalize to the scenes with more sub-distributions. \square

Theorem 2. *In the training process, nonuniform sampling is more likely to occur when one or several sub-distributions are dominating in the sampling of p_{data} in the training process.*

Proof. Use $\mathbf{x} \in p$ to represent \mathbf{x} is sampled from distribution p . Let the sub-distributions $\phi_s = \{\phi_m, \phi_{m+1}, \dots, \phi_n\}$ to be dominating in p_{data} in the sampling of training, where $1 \leq m \leq n \leq K$ and $n - m < K - 1$. Then it is equivalent to the situation that $P(\mathbf{x}_i \in \phi_s | \mathbf{x}_i \in p_{data}) \rightarrow 1$. Then in a data batch, we will have

$$\sum_{i=1}^b P(\mathbf{x}_i \in \phi_s | \mathbf{x}_i \in p_{data}) \rightarrow 1. \quad (7)$$

According to the definition, nonuniform sampling is more likely to occur. \square

Corollary 1. *In the training process, a large batch size can alleviate the nonuniform sampling problem.*

Proof. According to the proof of Theorem 2, the probability that all samples are from ϕ_s is

$$\prod_{i=1}^b P(\mathbf{x}_i \in \phi_s | \mathbf{x}_i \in p_{data}) \quad (8)$$

Because the range of $P(\mathbf{x}_i \in \phi_s | \mathbf{x}_i \in p_{data})$ is $(0, 1)$, the probability of nonuniform sampling reduces with a larger b . \square

At the points where nonuniform sampling occurs, $C(G)$ will be more likely to reach the minimum when $p_g \neq p_{data}$. Therefore, there will be more risks of mode collapse. We consider that most distributions contain linearly combined parts, so nonuniform sampling is one reason for mode collapse, and we will try to alleviate this problem.

IV. METHOD

A. Motivation

As mentioned above, some samples can make $C(G)$ reach or be close to the minimum value when $p_g \neq p_{data}$. They are like pits on a flat surface, and we will try to fix them to combat mode collapse.

In the theoretical design of GAN frameworks, the virtual training criterion for the generator is a distance that reaches the minimum when $p_g = p_{data}$. However, when nonuniform sampling occurs, the network's vision is limited to p_s . No matter how accurate the method we use, only $p_g = p_s$ can be achieved because p_{data} is unknown in this iteration. To alleviate this problem, trying to incorporate information of p_{data} into each training iteration should be effective. Based on this idea, we propose two distribution fitting methods aiming at different conditions.

B. Global Distribution Fitting

A direct method is to estimate the overall real distribution, and require the generated distribution to match it. However, the distributions are usually complicated, whose probability density functions are difficult to represent. Meanwhile, estimating the overall generated distribution in training will also be time-consuming. Thus, we consider only involving some critical information instead of the overall distribution. For a distribution, the mean and standard deviation are critical parameters. Global distribution fitting (GDF) is a method of adding a penalty term to constrain the means and standard deviations. First, we calculate the mean and standard deviation of each point of the overall real data before training, which are represented as $\boldsymbol{\mu}_r = \{\mu_{r1}, \mu_{r2}, \dots, \mu_{rn}\}$ and $\boldsymbol{\sigma}_r = \{\sigma_{r1}, \sigma_{r2}, \dots, \sigma_{rn}\}$ for n -tuple data. Second, in the training process, the generator will generate a mini-batch data whose mean and standard deviation are $\boldsymbol{\mu}_g = \{\mu_{g1}, \mu_{g2}, \dots, \mu_{gn}\}$ and $\boldsymbol{\sigma}_g = \{\sigma_{g1}, \sigma_{g2}, \dots, \sigma_{gn}\}$. We use $\boldsymbol{\mu}_g$ and $\boldsymbol{\sigma}_g$ to match the mean and standard deviation of p_g . Then the penalty term is defined as

$$\mathbb{L}(G) = \frac{1}{n} [\|\boldsymbol{\mu}_g - \boldsymbol{\mu}_r\|_1 + \|\boldsymbol{\sigma}_g - \boldsymbol{\sigma}_r\|_1] \quad (9)$$

It is expected to be minimized by the generator, which is independent of the adversarial training. The total training objective is

$$\min_G [\max_D V(D, G) + \lambda \mathbb{L}(G)] \quad (10)$$

λ is the weight of the penalty term. We set it to 1 in experiments because its value will not have significant impacts on the properties of GDF. Then we will prove that GDF will not change the global minimum of the GAN objective and that it can suppress the nonuniform sampling issue. Two lemmas are introduced at first.

Lemma 2. For a function $f(x) = f_1(x) + f_2(x)$, $f(x)$ must be bounded below if $f_1(x)$ and $f_2(x)$ are both bounded below.

Proof. Assume $f_1(x) \geq M$ and $f_2(x) \geq N$, then there must be $f(x) \geq M + N$. Therefore, $f(x)$ must be bounded below. \square

Lemma 3. For a function $f(x) = f_1(x) + f_2(x)$ where $f_1(x)$ and $f_2(x)$ are both bounded below, if $f_1(x)$ and $f_2(x)$ can reach the minimum simultaneously, $f(x)$ will reach the minimum if and only if $f_1(x)$ and $f_2(x)$ reach the minimum simultaneously.

Proof. Assume $f_1(x) \geq M$ and $f_2(x) \geq N$, then there must be $f(x) \geq M + N$. If there exists x which make $f_1(x) = M$ and $f_2(x) = N$, we will have $f(x) = M + N$, which is the minimum. Therefore, $f(x)$ will reach the minimum if $f_1(x)$ and $f_2(x)$ reach the minimum simultaneously.

Assume there exists x which makes $f(x) = M + N$ when $f_1(x)$ and $f_2(x)$ do not reach the minimum simultaneously. Then there must be $f_1(x) > M$ or $f_2(x) > N$. If $f_1(x) > M$, we have

$$\begin{aligned} f_2(x) &= M + N - f_1(x) \\ &= N + [M - f_1(x)] \\ &< N \end{aligned} \quad (11)$$

which is contrary with $f_2(x) \geq N$. If $f_2(x) > N$, similarly we have $f_1(x) < M$ which is contrary with $f_1(x) \geq M$. Therefore, $f(x)$ will reach the minimum only if $f_1(x)$ and $f_2(x)$ reach the minimum simultaneously. \square

Then we will prove the effectiveness of GDF. Because $C(G) = \max_D V(D, G)$, for simplicity, let $C^*(G) = C(G) + \lambda \mathbb{L}(G)$.

Theorem 3. If and only if $p_g = p_{data}$, $C^*(G)$ can reach the global minimum.

Proof. We know that $C(G)$ is bounded below according to [13]. In the calculation of $\mathbb{L}(G)$, the 1-norm is non-negative. According to Lemma 2, $\mathbb{L}(G)$ is bounded below. Then for $C^*(G)$, $C(G)$ and $\mathbb{L}(G)$ are both bounded below. According to Lemma 2, $C^*(G)$ is also bounded below.

The minimum of $C(G)$ is reached when $p_g = p_{data}$ according to [13]. For $\mathbb{L}(G)$, 1-norm will reach the minimum 0 when all the elements in the vector is zero. And because it is possible that $\boldsymbol{\mu}_g = \boldsymbol{\mu}_r$ and $\boldsymbol{\sigma}_g = \boldsymbol{\sigma}_r$ simultaneously, the minimum of $\mathbb{L}(G)$ is 0 according to Lemma 3. Then because it is possible that $p_g = p_{data}$, $\boldsymbol{\mu}_g = \boldsymbol{\mu}_r$ and $\boldsymbol{\sigma}_g = \boldsymbol{\sigma}_r$ exist simultaneously, $C^*(G)$ can reach the minimum according to Lemma 3.

According to Lemma 3, $C^*(G)$ will reach the minimum only if $C(G)$ and $\mathbb{L}(G)$ reach the minimum simultaneously. According to [13], $C(G)$ will reach the minimum only if $p_g = p_{data}$. Therefore, $C^*(G)$ will reach the minimum only if $p_g = p_{data}$. \square

According to Theorem 3, the global minimum of the GAN training objective is not changed with GDF. For other GAN frameworks with different objectives, the theorem is also effective because they still reach the minimum if and only if $p_g = p_{data}$. Thus, there are no negative effects for GANs with our method.

Theorem 4. *If nonuniform sampling occurs, $C^*(G)$ can reach the minimum only if the means of all sub-distributions of p_{data} can be linearly expressed by basic solutions*

$$(\xi_1, \xi_2, \xi_3, \dots, \xi_n) = \begin{pmatrix} A \\ E \end{pmatrix} \quad (12)$$

where E is an $n - 1$ dimension identity matrix. A is a row vector

$$\left(-\frac{\alpha_2}{\alpha_1}, -\frac{\alpha_3}{\alpha_1}, \dots, -\frac{\alpha_m - \beta_m}{\alpha_1}, \dots, -\frac{\alpha_n - \beta_n}{\alpha_1}, \dots, -\frac{\alpha_K}{\alpha_1} \right) \quad (13)$$

where α_k is the weight of the k -th sub-distribution of p_{data} , and β_k is the weight of the k -th sub-distribution of p_s .

Proof. Assuming that $C^*(G)$ reaches the minimum. First, $C(G)$ must reach the minimum according to Lemma 3. Then there must be $p_g = p_s$ because we use p_s to represent p_{data} in training. Therefore, we have $\mu_g = \mu_s$. Second, $\|\mu_g - \mu_r\|_1$ must be zero according to Lemma 3, which indicates $\mu_g = \mu_r$. As a result, we have $\mu_s = \mu_r$.

From Equations 4 and 5, we can calculate the means of p_{data} and p_s

$$\mu_r = \sum_{k=1}^K \alpha_k \mu_k \quad (14)$$

$$\mu_s = \sum_{k=m}^n \beta_k \mu_k \quad (15)$$

where μ_k is the mean of the k -th sub-distribution. With $\mu_s = \mu_r$, we have

$$\begin{aligned} \sum_{k=1}^K \alpha_k \mu_k &= \sum_{k=m}^n \beta_k \mu_k \\ \iff \alpha_1 \mu_1 + \alpha_2 \mu_2 + \dots + (\alpha_m - \beta_m) \mu_m + \dots \\ &+ (\alpha_n - \beta_n) \mu_n + \dots + \alpha_K \mu_K = 0 \end{aligned} \quad (16)$$

whose basic solution set is $(A^T, E)^T$. \square

It is not common that the means of the sub-distributions are in a certain proportional relationship, especially when β_k is not static and influenced by the sampling process. Therefore, according to Theorem 4, the minimum value is harder to be reached when $p_g \neq p_{data}$. Even if the sub-distributions are not linearly combined, the means should still be in a certain proportional relationship, and only the calculations in Eqs. 14 and 15 need to be changed. As a result, p_g will be more likely to converge to p_{data} , and mode collapse will be suppressed.

C. Local Distribution Fitting

In some circumstances, the real distribution is unknown or hard to calculate. For instance, if the real data is a black box and we can only sample from it, GDF will not work. It is because calculating the distribution parameters before training will be difficult, as it is almost impossible to define a general criterion of minimum training sample size [39] and we also cannot define the number of samples required for estimation. To cope with this situation, we propose a local distribution

fitting (LDF) method. It utilizes the mean μ_s and standard deviation σ_s of all sampled data in the previous training iterations to replace the real ones. In the training process, the penalty term is

$$\mathbb{L}_s(G) = \frac{1}{n} [\|\mu_g - \mu_s\|_1 + \|\sigma_g - \sigma_s\|_1] \quad (17)$$

and the training objective is

$$\min_G [\max_D V(D, G) + \lambda_s \mathbb{L}_s(G)] \quad (18)$$

λ_s is the weight which is also set to 1. When more and more data is sampled, μ_s and σ_s will be closer to the real ones. Then according to Theorems 3 and 4, p_g will be more likely to converge to p_{data} , and the mode collapse problem will also be suppressed.

V. EXPERIMENTS

In this section, we conduct experiments on the proposed methods. Several datasets will be involved, and the evaluation metrics will be introduced in each section.

A. Mixture of Gaussian Dataset

To illustrate the impact of distribution fitting, we train a simple network on a 2D mixture of 8 Gaussians arranged in a circle. Both the training setup and the network architecture are the same as those proposed by unrolledGAN [31], and we utilize an implementation of it¹ to conduct the experiment. The detailed network architecture is also provided in the Appendix. This experiment gives an intuitive result, which proves the effectiveness of GDF and LDF in suppressing mode collapse.

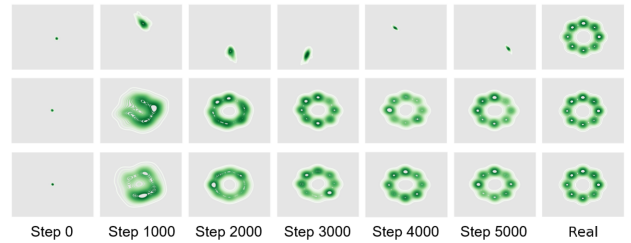


Fig. 1. The dynamics of the model through time. The image rows from top to bottom represent the model without distribution fitting, the model with LDF, and the model with GDF, respectively.

In Fig. 1, we observe that the original model suffers from severe mode collapse. Using GDF or LDF will inhibit mode collapse, and the network can learn a complete distribution. However, the difference between GDF and LDF is marginal. It is because the batch size is 512 in the training process. The real data only consists of eight sub-distributions, so the distribution of a generated batch is already very close to the global one.

There is also an extreme case where one Gaussian is dominating with a large weight while the others account for only a small part. Although the distribution of the 8 Gaussians is nonuniform with the training setup, this case is still hard

¹<https://github.com/andrewliao11/unrolled-gans>

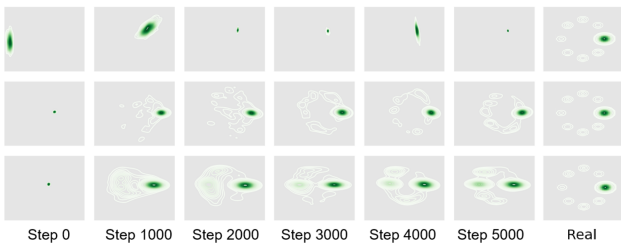


Fig. 2. The dynamics of the model through time in an extreme case. The image rows from top to bottom represent the model without distribution fitting, the model with LDF, and the model with GDF, respectively.

to reach. To demonstrate the effectiveness of GDF and LDF in this case, we manually set the weight of one Gaussian to 0.86, while the other seven weights are all 0.02. The training dynamics are illustrated in Fig. 2. With GDF or LDF, the network can also generate samples from the other sub-distributions, indicating that mode collapse is also suppressed.

B. Stacked MNIST Dataset

The effectiveness of suppressing mode collapse is frequently evaluated through experiments conducted on the stacked MNIST dataset. According to [5], the images in the stacked MNIST dataset are obtained by stacking three random single-channel images from MNIST [21]. Therefore, there are 1,000 modes that need to be generated. In practice, the stacked images are produced dynamically in the training process. As there are too many possible stacked images, the real mean and standard deviation cannot be calculated before training. Therefore, GDF is not available.

In order to demonstrate the effectiveness of both GDF and LDF, we first make a static stacked MNIST dataset containing 60,000 images for training, so the mean and standard deviation of the real distribution can be calculated. Considering the practice is different from previous methods, we do not involve other frameworks for comparisons in this experiment. The baseline has a DCGAN-like architecture which is the same as the one proposed by [25], which has been provided in the Appendix. Each network will generate 25,600 samples, and we compute the predicted class label of each image channel by a pre-trained MNIST classifier². We report the number of modes for which at least one sample is generated. A higher mode number represents better results because it denotes that more modes are generated. We also report the Kullback-Leibler divergence (KL) between the generated samples and the real data over classes. A lower KL represents better results because it indicates that the generated distribution is more similar to the real one.

In TABLE I, the results illustrate two points. First, distribution fitting methods are effective in suppressing mode collapse. Learning a static dataset’s distribution is easier, so our baseline also achieves good performance. However, with GDF and LDF, generated modes are still noticeably increased, and the KL is also lower. Second, the results with GDF are only slightly better than those with LDF, which indicates that

TABLE I
EXPERIMENTS ON A STATIC STACKED MNIST DATASET THAT CONTAINS 60,000 IMAGES. THE RESULTS ARE AVERAGED OVER 10 TRIALS WITH STANDARD ERROR REPORTED. HIGHER MODES AND LOWER KL REPRESENT BETTER RESULTS.

GDF	LDF	Modes	KL
		876.8±3.69	0.40±0.006
✓		984.5±1.35	0.20±0.006
	✓	980.4±1.33	0.28±0.008

LDF can match the real distribution. Therefore, LDF is also effective for combating mode collapse.

Second, we produce the stacked images in the training process to fairly compare with other methods. As mentioned, the real distribution is unknown in this case, so only LDF is utilized.

TABLE II
EXPERIMENTS ON STACKED MNIST DATASET. MD DENOTES MINIBATCH DISCRIMINATION. THE LAST FOUR RESULTS ARE AVERAGED OVER 10 TRIALS WITH STANDARD ERROR REPORTED. HIGHER MODES AND LOWER KL REPRESENT BETTER RESULTS.

Method	Modes	KL
DCGAN [35]	99.0	3.40
ALI [9]	16.0	5.40
Unrolled GAN [31]	48.7	4.32
VEEGAN [41]	150.0	2.95
MD [15]	24.5±7.67	5.49±0.418
PacDCGAN2 [25]	1000.0±0.00	0.06±0.003
Baseline	24.1±4.10	7.48±0.998
Baseline w/ LDF	970.0±2.28	0.23±0.020

In TABLE II, the first six rows are directly copied from [25]. It is obvious that LDF achieves competitive performance. However, the performance does not reach the best, which is not as good as PacDCGAN2 [25]. We consider that it is because the batch size is not large enough. In LDF, the mean and standard deviation of generated data will be matched by those of a batch. Therefore, we consider that a large batch size will benefit LDF. To validate the hunch, we use different batch sizes to train the models.

TABLE III
EXPERIMENTS ON STACKED MNIST DATASET WITH DIFFERENT BATCH SIZES. THE RESULTS ARE AVERAGED OVER 10 TRIALS WITH STANDARD ERROR REPORTED. HIGHER MODES AND LOWER KL REPRESENT BETTER RESULTS.

Batch Size	Method	Modes	KL
1x	Baseline	24.1±4.10	7.48±0.998
	Baseline w/ LDF	970.0±2.28	0.23±0.020
10x	Baseline	157.0±71.50	5.56±1.047
	Baseline w/ LDF	985.9±2.700	0.20±0.026
20x	Baseline	160.6±18.27	4.26±0.398
	Baseline w/ LDF	996.2±0.770	0.13±0.011
50x	Baseline	184.0±18.27	3.39±0.209
	Baseline w/ LDF	1000±0.000	0.03±0.002

In TABLE III, we see that with the increasing batch size, the performance will become better. It is proof of Corollary 1. Nevertheless, the larger batch size is not able to completely

²<https://github.com/fjxmlzn/PacGAN>

TABLE IV

EXPERIMENTS ON STACKED MNIST DATASET WITH DIFFERENT DISCRIMINATORS. THE RESULTS ARE AVERAGED OVER 10 TRIALS WITH STANDARD ERROR REPORTED. HIGHER MODES AND LOWER KL REPRESENT BETTER RESULTS.

Method	D is 1/4 size of G		D is 1/2 size of G	
	Modes	KL	Modes	KL
Unrolled GAN [31], 0 step	30.6±20.73	5.99±0.42	628.0±140.9	2.58±0.75
Unrolled GAN [31], 1 step	65.4±34.75	5.91±0.14	523.6±55.77	2.44±0.26
Unrolled GAN [31], 5 steps	236.4±63.30	4.67±0.43	732.0±44.98	1.66±0.09
Unrolled GAN [31], 10 steps	327.2±74.67	4.66±0.46	817.4±37.91	1.43±0.12
Baseline	77.4±28.37	8.66±1.34	394.6±79.31	2.40±0.64
Baseline w/ LDF	952.4±8.870	0.39±0.04	952.7±7.260	0.47±0.06

solve the mode collapse problem as the mode number is still less than 200, even with a 50x batch size. We can catch all 1,000 modes with LDF. Thus, LDF shows effectiveness with a large batch size.

As we mentioned that the weight of the penalty term is set to 1, we also conduct experiments to prove that its value will not have critical impacts. For simplicity, the experiments are conducted on the static dataset with 60,000 images and GDF. As shown in TABLE V, we consider that there are only some fluctuations in training. Thus, we believe the value of λ has no significant impact.

TABLE V

EXPERIMENTS ON A STATIC STACKED MNIST DATASET WITH DIFFERENT WEIGHTS OF THE PENALTY TERM. THE RESULTS ARE AVERAGED OVER 10 TRIALS WITH STANDARD ERROR REPORTED. HIGHER MODES AND LOWER KL REPRESENT BETTER RESULTS.

λ	Modes	KL
0.5	981.7±1.81	0.20±0.010
1.0	984.5±1.35	0.20±0.006
2.0	983.2±1.04	0.18±0.006

To prove the stability of LDF, experiments similar with [31] are conducted. We adjust the parameters of the discriminator to demonstrate the performance. In TABLE IV, the first four rows are from [31]. Obviously, our method achieves satisfactory performance, and it is still competitive with a weaker discriminator.

Finally, we give the convergence curves of the penalty term on the static dataset. From Eqs. 10 and 18, GDF and LDF will not be involved in the adversarial training but only be minimized by the generator. Thus, the penalty terms are expected to be kept at small values. The curves in Fig. 3 demonstrate that GDF and LDF are optimized as expected. Though LDF requires more iterations to estimate the parameters, it can finally be minimized similarly to GDF.

C. CIFAR-10, STL-10 and Tiny-ImageNet Dataset

Experiments on natural datasets are also necessary to demonstrate the effectiveness. We involve CIFAR-10 [20] and STL-10 [8], which are widely used, for our experiments. Additionally, considering our method is designed for combating mode collapse, we also involve Tiny-ImageNet [37], which contains 200 classes, to show the performance of our method on the multi-class generation task. In the experiments, each network will generate 25,600 images for testing.

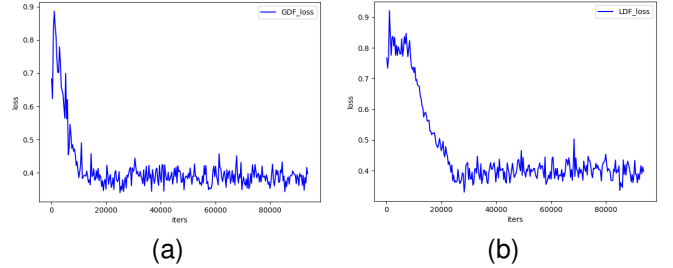


Fig. 3. The convergence curves of (a) GDF and (b) LDF. The horizontal coordinate axis represents the training iteration and the vertical one represents the values.

The Inception Score (IS) [40] and Fréchet Inception Distance (FID) [16] are reported. IS can be calculated with

$$IS(G) = \exp(E_{x \sim p_g} D_{KL}(p(y|x)||p(y))) \quad (19)$$

where p_g is the distribution of generated data, D_{KL} is the KL-divergence, x is the input image and y is the output of a pre-trained Inception V3 network [42]. A higher IS represents better results. FID can be calculated with

$$FID(y, g) = \|\mu_y - \mu_g\|_2^2 + Tr(\Sigma_y + \Sigma_g - 2(\Sigma_y \Sigma_g)^{\frac{1}{2}}) \quad (20)$$

where y and g are the outputs of a pre-trained Inception V3 network [42] with the real and generated data as the inputs, respectively. μ and Σ are the mean and covariance of the data distributions of y and g . FID represents the distance between the two datasets. We will calculate the FID between the generated data and the testing data, and a lower FID represents better results.

First, we evaluate our method with the original image resolutions. We also train some famous networks with a public implementation³ for comparisons. The results are shown in TABLE VI. We apply our GDF and LDF in GAN [13] and DCGAN [35] to demonstrate the effectiveness. We can observe that DCGAN with GDF achieves the best performance in most cases. Though the IS is not the best on CIFAR-10 and STL-10, the performance is still better than the original DCGAN. The comparisons prove that our method is effective. The convergence curves of GDF and LDF with DCGAN under different datasets can be found in Appendix.

Second, we try our method for higher image resolutions. As GAN [13] and DCGAN [35] are not designed for high-

³<https://github.com/eriklindernoren/PyTorch-GAN>

TABLE VI

EXPERIMENTS ON CIFAR-10, STL-10 AND TINY-IMAGENET. A HIGHER IS AND A LOWER FID REPRESENT BETTER RESULTS. THE SYMBOL * REPRESENTS THE METHOD DESIGNED FOR SUPPRESSING MODE COLLAPSE. THE SYMBOL † REPRESENTS THE RESULTS FOR COMPARISON OBTAINED FROM A MODEL TRAINED BY OURSELVES.

Method	CIFAR-10 (32 × 32)		STL-10 (32 × 32)		Tiny-ImageNet (64 × 64)	
	IS	FID	IS	FID	IS	FID
*MGGAN [2]	6.608	51.76	-	-	-	-
*MDGAN [10]	-	36.80	-	-	-	-
*D2GAN [33]	7.150±0.070	-	7.98	-	-	-
*DRAGAN [19]	6.900	68.50	-	-	-	-
BEGAN [3]	5.620	71.40	-	-	-	-
WGAN [1]	3.820±0.060	55.90	†3.764±0.042	†77.13	†3.419±0.044	†78.79
WGAN-GP [15]	6.680±0.060	40.20	8.420±0.130	55.10	†5.557±0.109	†66.45
DCGAN [35]	†6.474±0.045	†33.20	†7.744±0.055	†60.21	†5.315±0.100	†72.70
GAN [13]	†2.395±0.067	†89.98	†2.400±0.044	†93.31	†2.537±0.099	†90.01
*GAN w/ GDF (Ours)	2.986±0.029	85.78	2.563±0.047	82.24	2.549±0.065	88.44
*GAN w/ LDF (Ours)	2.904±0.030	85.11	2.498±0.015	86.74	2.537±0.087	89.12
*DCGAN w/ GDF (Ours)	6.965±0.077	30.03	7.991±0.095	53.24	6.002±0.078	65.19
*DCGAN w/ LDF (Ours)	6.798±0.081	30.23	7.826±0.079	55.26	5.875±0.089	70.58

TABLE VII

EXPERIMENTS ON CIFAR-10, STL-10 AND TINY-IMAGENET WITH HIGHER RESOLUTIONS. A HIGHER IS AND A LOWER FID REPRESENT BETTER RESULTS.

Method	Size	CIFAR-10		STL-10		Tiny-ImageNet	
		IS	FID	IS	FID	IS	FID
StyleGAN2 [17]	128 × 128	8.266±0.094	8.80	8.660±0.212	9.64	10.082±0.222	12.31
StyleGAN2 w/ GDF (Ours)		8.517±0.092	8.70	8.801±0.217	9.42	10.134±0.219	10.12
StyleGAN2 w/ LDF (Ours)		8.398±0.101	8.68	8.777±0.202	9.46	10.134±0.237	10.66
StyleGAN2 [17]	256 × 256	9.143±0.142	9.68	9.446±0.179	10.46	10.371±0.429	12.69
StyleGAN2 w/ GDF (Ours)		9.221±0.118	9.56	9.508±0.152	10.29	10.522±0.375	10.04
StyleGAN2 w/ LDF (Ours)		9.201±0.131	9.61	9.495±0.150	10.46	10.498±0.343	10.38

resolution generation, we involve StyleGAN2 [17] to generate larger images. The results are shown in TABLE VII.

D. Visualization

The generated samples on MNIST [21], CIFAR-10 [20], STL-10 [8] and Tiny-ImageNet [37] are visualized to give a intuitive result.

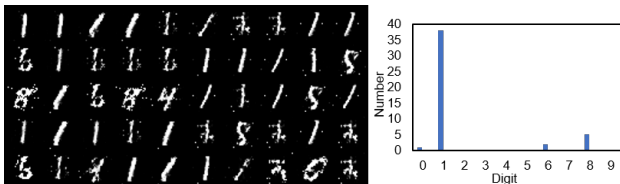


Fig. 4. The samples in a mini-batch generated by GAN on MNIST, and the number of samples per class in the mini-batch.

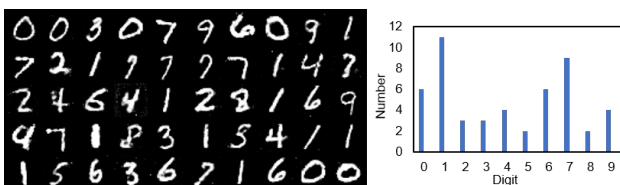


Fig. 5. The samples in a mini-batch generated by GAN with GDF on MNIST, and the number of samples per class in the mini-batch.

In Fig. 4, we visualize the generated samples in a mini-batch of the original GAN [13] framework. We see in the histogram that most samples contain the digit 1, which indicates that mode collapse occurs. In Fig. 5, we visualize the generated samples of the framework trained with GDF, which illustrates that mode collapse has been suppressed.

In Figs. 6, 7, and 8, some generated samples on CIFAR-10, STL-10, Tiny-ImageNet are visualized. It can be observed that DCGAN [35] can reach a better performance with GDF.

E. Efficiency

We assert that the computation and time cost of GDF and LDF can almost be ignored. Thus, the floating point operations (FLOPs) and time cost are discussed. For GDF, the overall mean and standard deviation of real data are required, but they can be calculated before training. Then the values can be saved as a part of the dataset, so repeated calculation is not necessary. Therefore, the computation cost of GDF is less than LDF, and we will mainly discuss LDF.

In one training iteration, LDF requires the calculation of the means and standard deviations of a batch of generated data and all previous real data. Taking DCGAN [35] trained on CIFAR-10 [20] as an example, we will try to compute the parameters.

The generated data has four dimensions, and the size is (128, 3, 32, 32), representing the batch size, the number of channels, the width, and the height, respectively. First, the



Fig. 6. The samples in a mini-batch generated by DCGAN (left), DCGAN with LDF (middle), and DCGAN with GDF (right) on CIFAR-10.

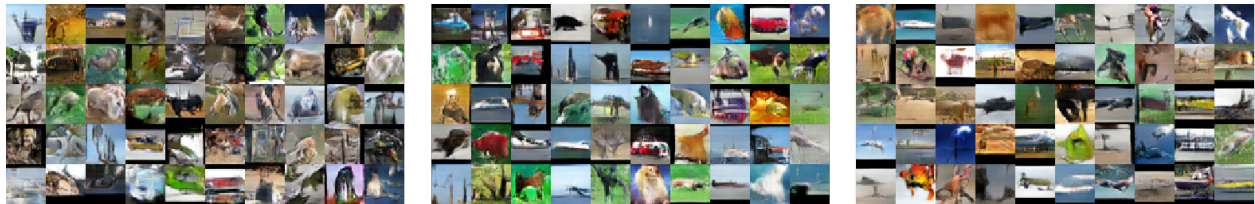


Fig. 7. The samples in a mini-batch generated by DCGAN (left), DCGAN with LDF (middle), and DCGAN with GDF (right) on STL-10.



Fig. 8. The samples in a mini-batch generated by DCGAN (left), DCGAN with LDF (middle), and DCGAN with GDF (right) on Tiny-ImageNet.

means will be calculated on the first dimension in our design, which contains 128 values for one mean. Therefore, it takes 127 add operations and 1 division operation. There are a total of $3 \times 32 \times 32 = 3072$ means, so the generated ones will take 393.216K FLOPs. Second, one standard deviation will also be calculated with 128 values. It takes 128 add operations to subtract the mean, 128 multiplication operations to get the square, 127 add operations to sum the results, 1 division operation, and 1 square root operation. There are also 3072 standard deviations, so the generated ones will take about 1.183M FLOPs.

As for the real data, the previous means and standard deviations are recorded. With a new batch of data, one mean takes 1 multiplication operation to get the sum of previous values, 128 add operations to get the new sum, and 1 division operation. As a result, the means of the real data will take 399.36K FLOPs. One standard deviation will take 2 multiplication operations to get the previous sum, 128 add operations to subtract the mean, 128 multiplication operations to get the square, 128 add operations to get the new sum, 1 division operation, and 1 square root operation. As a result, the standard deviations of the real data will take about 1.192M FLOPs.

In the training process, the means and standard deviations for real and generated data will both be calculated once in one iteration. To summarize, LDF will take about 3.167M FLOPs in one training iteration. As mentioned, GDF will take fewer FLOPs. In comparison, one front propagation of DCGAN [35] will consume more than 14G FLOPs. Therefore, we argue that the computation cost of our method can almost be ignored. However, the efficiency may be affected by the batch size

and number of data elements. The computation complexity is $O(mn)$ for n -tuple data where m is the batch size. Thus, the complexity is proportional to the product of the batch size and the data element number.

To further demonstrate that the cost is very small, we record the training time of DCGAN [35], where CIFAR-10 [20] provides the data. The results are shown in TABLE VIII. It can be observed that the training time is not increased noticeably, which proves that the time cost of our method is small.

TABLE VIII
TRAINING TIME OF DCGAN. THE MODELS ARE TRAINED ON CIFAR-10 FOR 200 EPOCHS. PER CALC. REPRESENTS THE TIME FOR CALCULATING THE PROPOSED PENALTY IN ONE ITERATION.

Method	Total	Per Epoch	Per Iteration	Per Calc.
DCGAN [35]	5830.6s	29.2s	0.04s	0.00ms
DCGAN w/ GDF	5892.0s	29.5s	0.04s	0.26ms
DCGAN w/ LDF	5909.3s	29.5s	0.04s	0.39ms

VI. DISCUSSION

We will discuss the advantages and limitations of our method. In the same way that for the commonly used regularization methods, the main advantage of our method is that no manual design is required. Many techniques for combating mode collapse tried to force the generator to generate diverse data. These approaches will need to be modified for a decent performance if a dataset contains data that is not diverse originally. Thus, the adaptability for various scenes of our method is better.

Compared to regularization methods, our method has two advantages. First, GDF and LDF only need a small amount of computation. The number of latent nodes in a network is usually much higher than the input layer. Therefore, compared to editing gradients in each latent node, our method requires less computation. Second, GDF and LDF are independent of the front propagation process, so they are easy to be transplanted. The distribution parameters are calculated independently, and only a penalty term is provided to be added to the training objective. In comparison, some regularization methods require changing the gradients in the front propagation process, which is more difficult to be applied in different frameworks.

Nevertheless, the limitation of our method is also obvious. First, because we utilize the mean and standard deviation of a batch to match those of the generated distribution, a large batch size must be applied. In some applications, the method will not work. For instance, for unpaired image-to-image translation, the batch size is usually set to 1 to achieve the best performance. For high-resolution image synthesis, sometimes, a single GPU can only deal with one image. Second, the mean and standard deviation only convey partial information, which is not enough to represent a distribution, especially for high-dimensional ones. Therefore, the applications may be limited, so we consider finding a better representation of data composition, e.g., using kernel density estimation, is valuable in the future. Last, we only demonstrate the effectiveness of our method when the sub-distributions are linearly combined. Although the experiments prove that it is most likely correct that most real distributions contain linear parts, the possible effectiveness of non-linearly combined mixed distributions is not thoroughly tested. In the future, exploring non-linearly combined mixed distributions may be valuable to refine our method.

VII. CONCLUSION

In this work, we analyze the causes of mode collapse in GANs. Then we propose a distribution fitting method to suppress mode collapse. We present GDF and LDF to cope with different situations, and the experiments demonstrate the effectiveness of our method. The method is simple and effective, and only a small amount of computation is required with no manual design. However, the requirement of a large batch size limits the applications. In the future, we consider identifying alternative representations of data composition and utilizing it to achieve distribution fitting will be valuable. It is also possible to integrate the method into the virtual training criterion for a novel distance representation between distributions. To accurately estimate the real distribution parameters, one more research interest is exploring the minimum sample size for achieving GDF. The works will also help GANs to be applied in more research fields.

ACKNOWLEDGMENTS

This work was supported in part by the National Key Research and Development Program of China with ID 2018AAA0103203.

APPENDIX

NETWORK IN MIXTURE OF GAUSSIAN EXPERIMENTS

The network is the same as the one utilized in [31]. We also provide the detailed architectures in TABLE IX and X.

TABLE IX
ARCHITECTURE OF THE GENERATOR IN MIXTURE GAUSSIAN EXPERIMENTS.

Layers	Input Channel	Output Channel
Fully Connected	256	128
ReLU	-	-
Fully Connected	128	128
ReLU	-	-
Fully Connected	128	2

TABLE X
ARCHITECTURE OF THE DISCRIMINATOR IN MIXTURE GAUSSIAN EXPERIMENTS.

Layers	Input Channel	Output Channel
Fully Connected	2	128
ReLU	-	-
Fully Connected	128	128
ReLU	-	-
Fully Connected	128	1
Sigmoid	-	-

NETWORK IN STACKED MNIST EXPERIMENTS

We use the DCGAN-like network utilized in PacGAN [25], which is different from the original DCGAN [35]. This network architecture can better represent mode collapse problems. The detailed architectures are shown in TABLE XI and XII. In the experiments of TABLE IV, the output channel number of each layer of the discriminator will be multiplied by $\frac{1}{2}$ or $\frac{1}{4}$.

TABLE XI
ARCHITECTURE OF THE GENERATOR IN STACKED MNIST EXPERIMENTS.
K, S, AND P REPRESENT KERNEL SIZE, STRIDE, AND PADDING SIZE.
CHANNELS SHOW THE INPUT-OUTPUT CHANNELS.

Layers	Configurations	Channels
Fully Connected	-	256-1024
Reshape	-	1024-64
Batch Normalization	-	-
ReLU	-	-
Transposed Convolution	{k3,s2,p1}	64-32
Batch Normalization	-	-
ReLU	-	-
Transposed Convolution	{k3,s2,p1}	32-16
Batch Normalization	-	-
ReLU	-	-
Transposed Convolution	{k3,s2,p1}	16-8
Batch Normalization	-	-
ReLU	-	-
Transposed Convolution	{k3,s1,p1}	8-3
Tanh	-	-

TRAINING SETUP OF EXPERIMENTS

In Section V.A, the training setup is as follows. The optimizers are Adam [18]. For the generator, the learning rate is 0.001. For the discriminator, the learning rate is 0.0001. The batch size is 512, and the network is trained for 5,000 iterations. The

TABLE XII
ARCHITECTURE OF THE DISCRIMINATOR IN STACKED MNIST EXPERIMENTS. K, S, AND P REPRESENT KERNEL SIZE, STRIDE, AND PADDING SIZE. CHANNELS SHOW THE INPUT-OUTPUT CHANNELS.

Layers	Configurations	Channels
Convolution	{k3, s2, p1}	3-8
Batch Normalization	-	-
Leaky ReLU	0.3	-
Convolution	{k3, s2, p1}	8-16
Batch Normalization	-	-
Leaky ReLU	0.3	-
Convolution	{k3, s2, p1}	16-32
Batch Normalization	-	-
Leaky ReLU	0.3	-
Reshape	-	32-512
Fully Connected	-	512-1
Sigmoid	-	-

experiments are carried out on a Linux platform with an Intel Core i7-8700 CPU, two USCORSAIR 16GB DDR4 RAMs, and an NVIDIA TITAN Xp GPU.

In Section V.B, the training setup is as follows. The optimizers are Adam [18] with a learning rate 0.0002. The original batch size is 128, and the network is trained for 200 epochs. The experiments are carried out on a Linux platform with an Intel Xeon(R) E5-2630 v3 CPU, four Samsung 16GB DDR4 RAMs, and three NVIDIA TITAN RTX GPUs.

In Section V.C, the training setup is as follows.

For GANs [13], DCGAN [35], WGAN [1] and WGAN-GP [15], the optimizers are Adam [18]. The learning rate is 0.001 for GANs, DCGAN, and WGAN-GP and 0.00005 for WGAN. The batch size is 128, and the networks are trained for 200 epochs. The experiments are carried out on a Linux platform with an Intel Xeon(R) E5-2630 v3 CPU, four Samsung 16GB DDR4 RAMs, and three NVIDIA TITAN RTX GPUs.

For StyleGAN2 [17], the optimizers are Adam [18] with a learning rate 0.002. The batch size is 64, and the networks are trained for 200000 iterations. The experiments are carried out on a Linux platform with an Intel Xeon(R) E5-2630 v3 CPU, four Samsung 16GB DDR4 RAMs, and three NVIDIA TITAN RTX GPUs.

CONVERGENCE CURVES ON NATURAL DATASETS

The convergence curves of GDF and LDF with DCGAN under different datasets are shown in Figs. 9, 10 and 11.

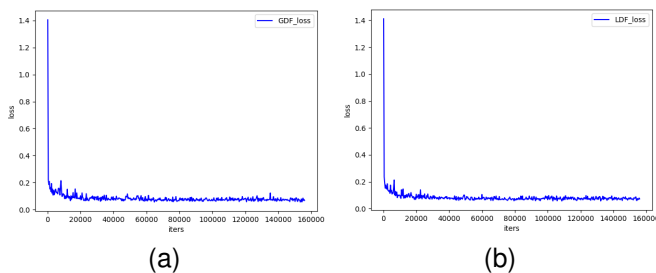


Fig. 9. The convergence curves of (a) GDF and (b) LDF on CIFAR-10. The horizontal coordinate axis represents the training iteration and the vertical one represents the values.

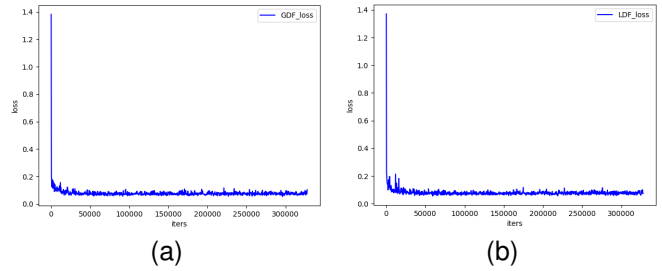


Fig. 10. The convergence curves of (a) GDF and (b) LDF on STL-10. The horizontal coordinate axis represents the training iteration and the vertical one represents the values.

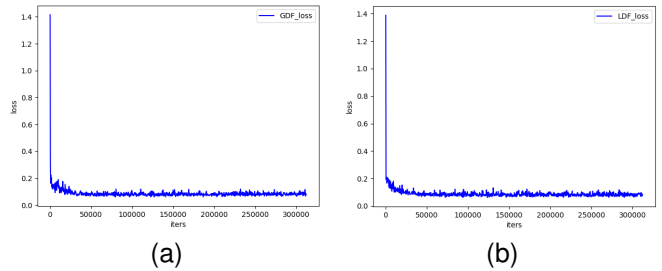


Fig. 11. The convergence curves of (a) GDF and (b) LDF on Tiny-ImageNet. The horizontal coordinate axis represents the training iteration and the vertical one represents the values.

The penalty terms are minimized as expected, proving the effectiveness.

REFERENCES

- [1] Martin Arjovsky, Soumith Chintala, and Léon Bottou. Wasserstein generative adversarial networks. In *International Conference on Machine Learning*, pages 214–223, 2017.
- [2] Duhyeon Bang and Hyunjung Shim. MGGAN: Solving mode collapse using manifold-guided training. In *Proceedings of the IEEE/CVF International Conference on Computer Vision*, pages 2347–2356, 2021.
- [3] David Berthelot, Thomas Schumm, and Luke Metz. BEGAN: Boundary equilibrium generative adversarial networks. *arXiv preprint arXiv:1703.10717*, 2017.
- [4] Andrew Brock, Jeff Donahue, and Karen Simonyan. Large scale GAN training for high fidelity natural image synthesis. In *International Conference on Learning Representations*, 2018.
- [5] Tong Che, Yanran Li, Athul Paul Jacob, Yoshua Bengio, and Wenjie Li. Mode regularized generative adversarial networks. *arXiv preprint arXiv:1612.02136*, 2016.
- [6] Yunjey Choi, Youngjung Uh, Jaejun Yoo, and Jung-Woo Ha. StarGAN v2: Diverse image synthesis for multiple domains. In *Proceedings of the IEEE/CVF Conference on Computer Vision and Pattern Recognition*, pages 8188–8197, 2020.
- [7] Penny Chong, Lukas Ruff, Marius Kloft, and Alexander Binder. Simple and effective prevention of mode collapse in deep one-class classification. In *2020 International Joint Conference on Neural Networks*, pages 1–9. IEEE, 2020.
- [8] Adam Coates, Andrew Ng, and Honglak Lee. An analysis of single-layer networks in unsupervised feature learning. In *Proceedings of the Fourteenth International Conference on Artificial Intelligence and Statistics*, pages 215–223, 2011.
- [9] Vincent Dumoulin, Ishmael Belghazi, Ben Poole, Olivier Mastropietro, Alex Lamb, Martin Arjovsky, and Aaron Courville. Adversarially learned inference. *arXiv preprint arXiv:1606.00704*, 2016.
- [10] Hamid Eghbal-zadeh, Werner Zellinger, and Gerhard Widmer. Mixture density generative adversarial networks. In *Proceedings of the IEEE/CVF Conference on Computer Vision and Pattern Recognition*, pages 5820–5829, 2019.

- [11] Pengfei Ge, Chuan-Xian Ren, Dao-Qing Dai, Jiashi Feng, and Shuicheng Yan. Dual adversarial autoencoders for clustering. *IEEE Transactions on Neural Networks and Learning Systems*, 31(4):1417–1424, 2019.
- [12] Arnab Ghosh, Viveka Kulharia, Vinay P Namboodiri, Philip HS Torr, and Puneet K Dokania. Multi-agent diverse generative adversarial networks. In *Proceedings of the IEEE Conference on Computer Vision and Pattern Recognition*, pages 8513–8521, 2018.
- [13] Ian Goodfellow, Jean Pouget-Abadie, Mehdi Mirza, Bing Xu, David Warde-Farley, Sherjil Ozair, Aaron Courville, and Yoshua Bengio. Generative adversarial nets. *Advances in Neural Information Processing Systems*, 27, 2014.
- [14] Aditya Grover, Jiaming Song, Ashish Kapoor, Kenneth Tran, Alekh Agarwal, Eric J Horvitz, and Stefano Ermon. Bias correction of learned generative models using likelihood-free importance weighting. *Advances in Neural Information Processing Systems*, 32, 2019.
- [15] Ishaan Gulrajani, Faruk Ahmed, Martin Arjovsky, Vincent Dumoulin, and Aaron C Courville. Improved training of wasserstein GANs. *Advances in Neural Information Processing Systems*, 30, 2017.
- [16] Martin Heusel, Hubert Ramsauer, Thomas Unterthiner, Bernhard Nessler, and Sepp Hochreiter. GANs trained by a two time-scale update rule converge to a local nash equilibrium. *Advances in Neural Information Processing Systems*, 30, 2017.
- [17] Tero Karras, Samuli Laine, Miika Aittala, Janne Hellsten, Jaakko Lehtinen, and Timo Aila. Analyzing and improving the image quality of StyleGAN. In *Proceedings of the IEEE/CVF Conference on Computer Vision and Pattern Recognition*, pages 8110–8119, 2020.
- [18] Diederik P Kingma and Jimmy Ba. Adam: A method for stochastic optimization. *arXiv preprint arXiv:1412.6980*, 2014.
- [19] Naveen Kodali, Jacob Abernethy, James Hays, and Zolt Kira. On convergence and stability of GANs. *arXiv preprint arXiv:1705.07215*, 2017.
- [20] Alex Krizhevsky. Learning multiple layers of features from tiny images. *Master's thesis, University of Toronto*, 2009.
- [21] Yann LeCun, Léon Bottou, Yoshua Bengio, and Patrick Haffner. Gradient-based learning applied to document recognition. *Proceedings of the IEEE*, 86(11):2278–2324, 1998.
- [22] Cheng-Han Lee, Ziwei Liu, Lingyun Wu, and Ping Luo. MaskGAN: Towards diverse and interactive facial image manipulation. In *Proceedings of the IEEE/CVF Conference on Computer Vision and Pattern Recognition*, pages 5549–5558, 2020.
- [23] Wei Li, Li Fan, Zhenyu Wang, Chao Ma, and Xiaohui Cui. Tackling mode collapse in multi-generator GANs with orthogonal vectors. *Pattern Recognition*, 110:107646, 2021.
- [24] Jae Hyun Lim and Jong Chul Ye. Geometric GAN. *arXiv preprint arXiv:1705.02894*, 2017.
- [25] Zinan Lin, Ashish Khetan, Giulia Fanti, and Sewoong Oh. PacGAN: The power of two samples in generative adversarial networks. *Advances in Neural Information Processing Systems*, 31, 2018.
- [26] Kanglin Liu, Wenming Tang, Fei Zhou, and Guoping Qiu. Spectral regularization for combating mode collapse in GANs. In *Proceedings of the IEEE/CVF International Conference on Computer Vision*, pages 6382–6390, 2019.
- [27] Rui Liu, Yixiao Ge, Ching Lam Choi, Xiaogang Wang, and Hongsheng Li. Divco: Diverse conditional image synthesis via contrastive generative adversarial network. In *Proceedings of the IEEE/CVF Conference on Computer Vision and Pattern Recognition*, pages 16377–16386, 2021.
- [28] Steven Liu, Tongzhou Wang, David Bau, Jun-Yan Zhu, and Antonio Torralba. Diverse image generation via self-conditioned GANs. In *Proceedings of the IEEE/CVF Conference on Computer Vision and Pattern Recognition*, pages 14286–14295, 2020.
- [29] Qi Mao, Hsin-Ying Lee, Hung-Yu Tseng, Siwei Ma, and Ming-Hsuan Yang. Mode seeking generative adversarial networks for diverse image synthesis. In *Proceedings of the IEEE/CVF Conference on Computer Vision and Pattern Recognition*, pages 1429–1437, 2019.
- [30] Lars Mescheder, Andreas Geiger, and Sebastian Nowozin. Which training methods for GANs do actually converge? In *International Conference on Machine Learning*, pages 3481–3490, 2018.
- [31] Luke Metz, Ben Poole, David Pfau, and Jascha Sohl-Dickstein. Unrolled generative adversarial networks. In *International Conference on Learning Representations*, 2016.
- [32] Takeru Miyato, Toshiki Kataoka, Masanori Koyama, and Yuichi Yoshida. Spectral normalization for generative adversarial networks. In *International Conference on Learning Representation*, 2018.
- [33] Tu Nguyen, Trung Le, Hung Vu, and Dinh Phung. Dual discriminator generative adversarial nets. *Advances in Neural Information Processing Systems*, 30, 2017.
- [34] Sen Pei, Richard Yi Da Xu, and Gaofeng Meng. dp-GAN: Alleviating mode collapse in GAN via diversity penalty module. *arXiv preprint arXiv:2108.02353*, 2021.
- [35] Alec Radford, Luke Metz, and Soumith Chintala. Unsupervised representation learning with deep convolutional generative adversarial networks. *arXiv preprint arXiv:1511.06434*, 2015.
- [36] Eitan Richardson and Yair Weiss. On GANs and GMMs. *Advances in Neural Information Processing Systems*, 31, 2018.
- [37] Olga Russakovsky, Jia Deng, Hao Su, Jonathan Krause, Sanjeev Satheesh, Sean Ma, Zhiheng Huang, Andrej Karpathy, Aditya Khosla, Michael Bernstein, et al. ImageNet large scale visual recognition challenge. *International Journal of Computer Vision*, 115(3):211–252, 2015.
- [38] Addison Salazar, Luis Vergara, and Gonzalo Safont. Generative adversarial networks and markov random fields for oversampling very small training sets. *Expert Systems with Applications*, 163:113819, 2021.
- [39] Addison Salazar, Luis Vergara, and Enrique Vidal. A proxy learning curve for the Bayes classifier. *Pattern Recognition*, 136:109240, 2023.
- [40] Tim Salimans, Ian Goodfellow, Wojciech Zaremba, Vicki Cheung, Alec Radford, and Xi Chen. Improved techniques for training GANs. *Advances in Neural Information Processing Systems*, 29, 2016.
- [41] Akash Srivastava, Lazar Valkov, Chris Russell, Michael U Gutmann, and Charles Sutton. VEEGAN: Reducing mode collapse in GANs using implicit variational learning. *Advances in Neural Information Processing Systems*, 30, 2017.
- [42] Christian Szegedy, Vincent Vanhoucke, Sergey Ioffe, Jon Shlens, and Zbigniew Wojna. Rethinking the inception architecture for computer vision. In *Proceedings of the IEEE Conference on Computer Vision and Pattern Recognition*, pages 2818–2826, 2016.
- [43] Ilya O Tolstikhin, Sylvain Gelly, Olivier Bousquet, Carl-Johann Simon-Gabriel, and Bernhard Schölkopf. AdaGAN: Boosting generative models. *Advances in Neural Information Processing Systems*, 30, 2017.
- [44] Ngoc-Trung Tran, Tuan-Anh Bui, and Ngai-Man Cheung. Dist-GAN: An improved GAN using distance constraints. In *Proceedings of the European Conference on Computer Vision*, pages 370–385, 2018.
- [45] Dong Wang, Xiaoqian Qin, Fengyi Song, and Li Cheng. Stabilizing training of generative adversarial nets via langevin stein variational gradient descent. *IEEE Transactions on Neural Networks and Learning Systems*, 33(7):2768–2780, 2020.
- [46] Haoran You, Yu Cheng, Tianheng Cheng, Chunliang Li, and Pan Zhou. Bayesian cycle-consistent generative adversarial networks via marginalizing latent sampling. *IEEE Transactions on Neural Networks and Learning Systems*, 32(10):4389–4403, 2020.
- [47] Ning Yu, Ke Li, Peng Zhou, Jitendra Malik, Larry Davis, and Mario Fritz. Inclusive GAN: Improving data and minority coverage in generative models. In *European Conference on Computer Vision*, pages 377–393, 2020.
- [48] Lei Zhao, Qihang Mo, Sihuan Lin, Zhizhong Wang, Zhiwen Zuo, Haibo Chen, Wei Xing, and Dongming Lu. UCTGAN: Diverse image inpainting based on unsupervised cross-space translation. In *Proceedings of the IEEE/CVF Conference on Computer Vision and Pattern Recognition*, pages 5741–5750, 2020.